Aerodynamic Design of Transonic Flying Wing Configurations

M. MEHEUT[1], R. GRENON[1], G. CARRIER[1], M. DEFOS[2] and M. DUFFAU[3]

[1]Applied Aerodynamics Department, Civil Aircraft Unit,
ONERA, Centre de Meudon, 8 rue des vertugadins, 92190 Meudon, France

[2]Aerodynamics Department,
Airbus France, 316 route de Bayonne, 31060 Toulouse Cedex 03, France.

[3]Future Project Office, Overal Aircraft Design,
Airbus France, 316 route de Bayonne, 31060 Toulouse Cedex 03, France.

Summary

This paper summarises the work carried out recently by ONERA and Airbus on flying wing configurations. The first part is dedicated to large capacity blended wing body configurations. The optimisation of a winglet equipped with a plain flap control surface on the VELA2 configuration is presented. This work was realised at ONERA within the framework of the European project NACRE to demonstrate the efficiency of such a winglet to decrease the total drag of the global configuration and to improve control and lateral stability. Substantial drag reduction and improvement on the control were obtained with the winglet in transonic conditions and in landing or take-off conditions. The second part is devoted to flying wing configurations of smaller capacity. Starting from a preliminary design worked out by the Airbus future project offices, an aerodynamic design work has been carried out within the context of the French project AVECA to achieve a configuration with satisfactory aerodynamic characteristics in transonic cruise conditions. With a precise target for the position of the center of pressure and lift coefficient, significant improvements of the trim, lift-to-drag ratio of the configuration were obtained in high speed conditions while achieving better pressure distributions with increased margin to detrimental transonic phenomena.

1 Introduction

The aerodynamic design of modern transport aircraft is driven primarily by cruise performance as well as regulation considerations. Indeed future environmental constraints will require significant reductions in emissions and noise pollution. Although the improvement of existing aircraft performance may provide a short term answer to this problem, the development of radically novel configurations is likely to be required to meet long term improvement objective. The flying wing or blended wing body seems to be one of the most promising configurations to reach a higher efficiency than current configurations, justifying the efforts recently devoted to flying wing configurations.

The first part of the paper is devoted to flying wing configurations for large capacity transonic transport. These configurations have been the subject of a renewed interest in the last decade within the framework of national and European projects [1-2]. Recently, ONERA has been involved in the European NACRE project which is an Integrated Project led by Airbus with a consortium of 36 partners and partly funded by the European Commission under the 6th Framework Program. The aim of this project is to develop technologies and design capabilities for new aircraft concepts and components, targeting a dramatic reduction in fuel burn and noise and substantial improvement in passenger comfort and economics. One of the activities of ONERA in this project is to define a winglet equipped with a control surface for flying wing configurations. The concept of a winglet with a plain flap control surface was studied numerically on the VELA2 configuration in order to demonstrate the efficiency of the winglet to improve the lift-to-drag ratio, the lateral stability and the control. The results obtained are presented in the first section of this paper with a precise description of the strategy used to define the winglet and of the results obtained in terms of drag and stability.

The second part of this paper is dedicated to the study of a flying wing configuration of smaller capacity. Past flying wing projects focused on large capacity aircraft and the application of the flying wing concept for smaller capacity aircraft has not been deeply evaluated. As a consequence, a national research project (AVECA) was launched on this subject. This project is carried out in close collaboration by Airbus and ONERA, and aims at designing viable flying wing geometries in terms of aerodynamic cruise performance while taking into account longitudinal trimming constraints and geometric constraints such as cabin or landing gear volumes. Some results of ONERA activity in the AVECA project are presented in this paper. First, a description of the methodology used to perform the aerodynamic design of the reference flying wing configuration is given. Then, the results of the aerodynamic analyses performed during the design and based on structured Navier-Stokes CFD computations are presented. These computations allowed to obtain a precise evaluation of the aerodynamic performance of the configuration with particular attention to the physical drag breakdown into viscous, wave and induced drag components.

2 Winglet design for large capacity flying wing configurations

2.1 Context

This first section presents the work carried out at ONERA, within the framework of the European NACRE project, on winglet design for the large capacity flying wing VELA2 configuration. This work aimed at modeling the effect produced on the control derivatives of the flying wing configuration by adding a device such as a winglet with a control flap. Indeed winglets are expected to provide a substantial drag reduction and an additional lateral stability. Moreover, due to the large span of the configuration, a control surface on the winglet is expected to increase yaw control and the desired level of control could be obtained with a limited size of the central fins.

2.2 Blended winglet concept

For several years, ONERA has worked on the blended winglet concept. Such winglets were optimised for heavy transport aircraft configurations or for light aircraft configurations. A blended winglet is generated by moving an airfoil section along curved spanwise directing lines and it may be considered as a smooth deformation of the original straight wing tip (figure 1). Such a shape allows having a large transversal curvature radius between the attachment section on the wing and the winglet tip, and this helps to avoid strong flow acceleration and possible flow separation at the wing-winglet junction, especially in transonic flow conditions.

However, if the winglet is supposed to have a unique trailing edge control surface, the main part of the winglet must be strictly a ruled surface so that the hinge line of the control surface could be a straight line. But a large blended fairing can be maintained between the attachment section on the wing and the root section of the ruled part of the winglet. A ruled winglet with a blended fairing was designed for the VELA 2 flying wing configuration using the parametrisation and the optimisation method and strategy presented in the following section.

2.3 Optimisation

2.3.1 Parametrisation of the winglet

The design method for a blended winglet is described in figure 1. In order to reduce the number of design variables, several parameters can be prescribed for the whole winglet (the span and the height) and for the ruled part (the dihedral angle, the root chord length, the tip chord length and the sweep angle of the trailing edge) to obtain a planform that should be suitable for transonic flow conditions. The generating airfoil can also be prescribed on the fairing and the ruled part. Nevertheless, up to 12 parameters are needed for the design of a blended winglet.

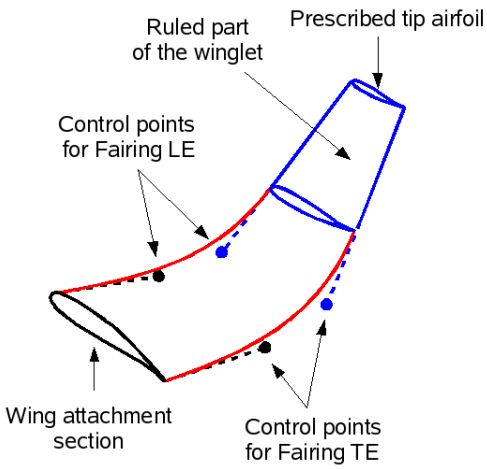

Figure 1 Design method for a blended winglet

The first two parameters are the angle of attack and the twist angle and law of the ruled part of the winglet. These two parameters define the position of the straight leading edge and of the straight trailing edge of the ruled part of the winglet. Then, four length parameters are needed to control the basic shape of the leading edge and of the trailing edge of the fairing considering geometrical constraints of tangency. Once the leading edge and the trailing edge are fully defined, the generating airfoil is propagated along the fairing and the ruled part of the winglet. The airfoil is usually interpolated according to the chord law between the airfoil at the wing attachment section and an airfoil that has been prescribed at the winglet tip section.

Six other parameters are used to control camber deformation only in three control sections: the middle section of the fairing where the transversal curvature is maximum, the end section of the fairing where the root section of the ruled part of the winglet is attached, and the tip section of the winglet. Then the camber deformation is interpolated along the whole winglet with the constraint that there is no deformation at the wing attachment section (figure 2).

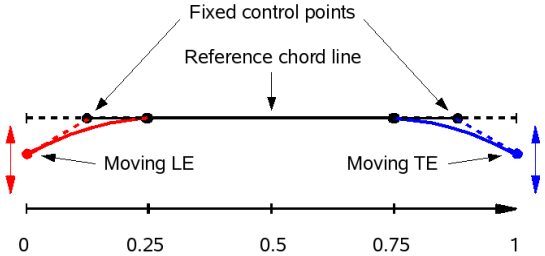

Figure 2 Camber deformation on a control section

Finally, a last control parameter is added to simulate the deflection of a plain flap type control surface at the trailing edge of the ruled part of the winglet. As the hinge line must be a straight line, a value of 25% can be used for the chordwise extension of the control surface to simulate moderate flap deflections where the flow should remain attached. As the flap deflection is limited to the ruled part of the winglet, there is a gap between the flap and the fairing when the flap is deflected, but in order to simplify the mesh generation, this gap is not taken into account. The shape of the winglet is always assumed to have no discontinuity and is smoothed around the gap when the flap is deflected.

2.3.2 Optimisation method

The optimisation method is based on the CONMIN code of G.N. Vanderplaats [3-4] which uses a gradient method (using finite differences) to perform the minimisation of the function of several variables under constraints. For aerodynamic optimisation, this software is coupled to a geometry generator, a fast algebraic mesh generator for structured grids, an Euler code for the aerodynamic computations and a module for constraints definition. The evaluation of the inviscid drag (sum of the induced and wave components) is carried out with the ONERA ffd code from Euler computations [5]. This code allows the elimination of the spurious drag due to numerical errors. As the Euler code does not provide the viscous drag, this component is evaluated using the flat plate boundary layer theory.

2.3.3 Optimisation strategy

The purpose of adding winglets on a flying wing is mainly to obtain more lateral control at landing and take-off conditions. As the winglet should not reduce the performance in cruise conditions, the optimisation process should take into account both low speed conditions and high speed conditions. But in order to reduce the computing time, the optimisation of the winglet was performed only in cruise conditions (Mach number 0.85, angle of attack 3° and altitude 35,000 feet) because transonic flow problems are thought to be the most critical ones.

The optimisation process of a winglet requires an initial shape having a suitable pressure distribution, which means smooth enough with not too high local Mach number values and not too strong shock waves. This initial shape was designed manually from previous experiences on similar winglet configurations. Then, the optimisation process was carried out with drag minimisation under constraints. A constraint was put on the maximum value allowed for the local Mach number at the upper side of the winglet but the lift was not constrained during the optimisation process.

When the convergence of the drag minimisation was reached, the maximum value of the local Mach number was chosen as the new objective function to be minimised and the drag value reached at the end of the drag minimisation became a constraint put on the maximum allowed value for the drag during the minimisation of the new objective function. Switching several times between the drag and the maximum value of the local Mach number as objective function and constraint allowed to overcome problem of incomplete convergence encountered with the gradient optimisation method and to further minimise both the drag and the maximum value of the local Mach number.

The final shape of the optimised winglet can be seen in figures 3 and 4 which show the iso-pressure curves obtained for transonic cruise conditions respectively with the clean winglet and with a 5° deflected control surface using the Euler code on a fine grid.

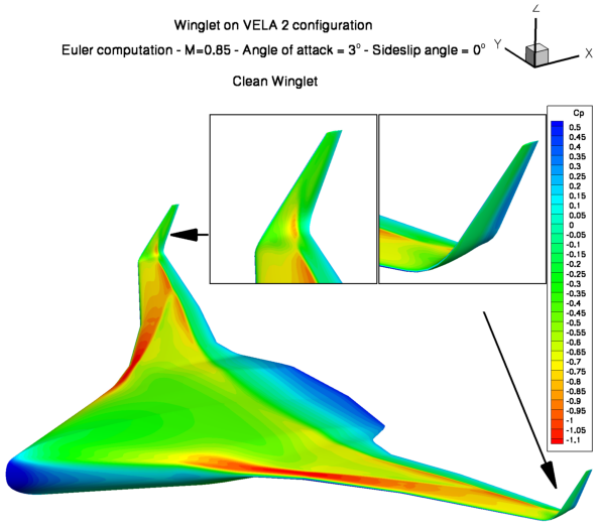

Figure 3 Euler computation on VELA2 with winglet and undeflected control surface

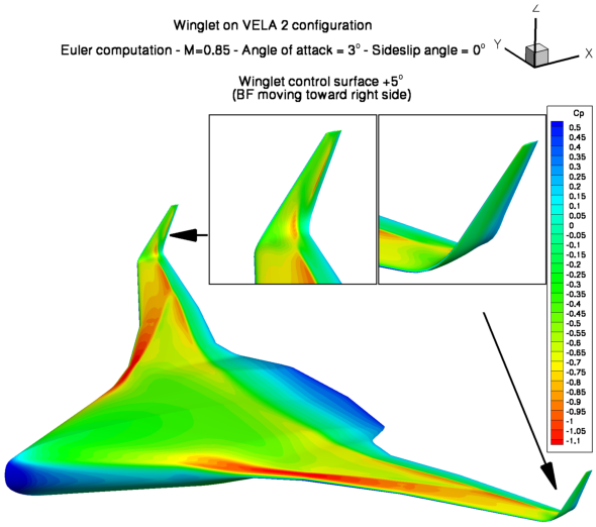

Figure 4 Euler computation on VELA2 with winglet and 5° deflected control surface

2.4 Performance analysis

2.4.1 Summary of the aerodynamic computations

The computations on the optimised VELA2 configuration were performed at low and transonic speed flight conditions. Table 1 summarises all the aerodynamic conditions used for the analysis of the reference configurationswithout winglet and of the configurations with winglet and undeflected control surface.

Mach number	***Angle of Attack***	***Sideslip Angle***	***Altitude***
0.85	3°	0° and 3°	35,000 feet
0.20	9°	0° and 3°	1,000 feet

Table 1 VELA2 configuration - Summary of the aerodynamic conditions

In the test cases above, all computations at zero sideslip angle were performed on a half aircraft but all computations at positive sideslip angle always needed to be performed on the full aircraft. Moreover, the configurations with winglet and deflected control surface were computed at the same Mach number and angle of attack conditions as shown above, but only at zero sideslip angle. These computations needed to be performed on a full aircraft with asymmetrical geometry because the goal was to obtain some yaw control; the deflection of the control surface was a 5° rotation moving its trailing edge towards the right side of the aircraft both for the left winglet and for the right winglet.

2.4.2 Winglet efficiency - Drag reduction

The comparison between the results of the reference configuration and of the corresponding configuration with a smooth winglet at zero sideslip angle gives the efficiency of the winglet for the drag reduction. Table 2 shows the relative differences between both configurations (winglet-reference) in terms of total drag (CD), induced drag (CDi), wave drag (CDw) and viscous drag (CDv) for both Mach numbers (0.2 and 0.85).

Mach number	***Angle of attack***	***ΔCD (%)***	***ΔCDi (%)***	***ΔCDw(%)***	***ΔCDv(%)***
0.2	9°	-2.45	-3.20	0.00	1.65
0.85	3°	-1.08	-3.18	3.12	1.65

Table 2 VELA2 configuration – Winglet efficiency and drag reduction

This table underlines that the influence of the winglet is identical for both Mach numbers on the induced and viscous drag components. However for the transonic case, the winglet is responsible for an important increase of the wave drag what explains that the efficiency of the winglet in terms of total drag is more important for the lowest Mach number.

2.4.3 Winglet efficiency – Lateral derivatives

The comparison between the results at zero sideslip angle and the results at positive sideslip angle for a given configuration gives the lateral derivatives of its aerodynamic coefficients. As the flat plate theory does not take into account the angle of attack or the sideslip angle, the rough estimation of the viscous drag at positive sideslip angle is assumed to be identical to the value at zero sideslip angle. The lateral derivatives of the aerodynamic coefficients (C* β) are defined as the difference value at some sideslip angle minus the value at zero sideslip angle divided by the sideslip in radians. Table 3 summarises the results for the rolling (Cl) and yawing (Cn) moments for both configurations.

Mach number	***Angle of attack***	***Configuration***	***Cl β***	***Cn β***
0.2	9°	Reference	-0.2607	-0.0186
		Winglet	-0.3027	-0.0094
0.85	3°	Reference	-0.3528	-0.0154
		Winglet	-0.4315	0.0322

Table 3 VELA2 configuration – Winglet efficiency and lateral derivatives

Lateral stability requires the rolling moment derivative Cl β to be negative and the yawing moment derivative Cn β to be positive. Thus, for a positive sideslip angle, the relative wind comes from the right of the aircraft and lateral stability requires the right wing to move upward and backward in order to reduce the sideslip angle. Table 3 shows that

the winglet has a positive effect on the lateral stability by increasing the magnitude of the stable negative rolling moment derivative for both Mach number and by recovering some yaw stability with a positive yawing moment derivative Cn β for the highest Mach number. For the lowest Mach number the winglet improves the yaw control but the configuration remains unstable. It should be noted that the VELA2 configuration was designed to have vertical fins which provide lateral stability whereas the winglet design was undertaken with a modified VELA2 configuration without fins.

2.4.4 Control surface efficiency

The efficiency of the winglet's control surface is computed by comparing the results with the smooth winglet and the results with the deflected control surface. An asymmetric deflection is always assumed, so that a positive deflection of the control surface moves its trailing edge toward the right side of the aircraft on the left winglet as well as on the right winglet. As the load of each winglet points toward the symmetry plane, a positive deflection of the control surface increases the load of the right winglet and decreases the load of the left winglet. The difference between the normal load of the left winglet and the normal load of the right winglet when the control surface is deflected is expected to give both roll and yaw control. Moreover, the drag of each winglet is expected to increase or decrease like its normal load, thus giving additional yaw control.

The deflection of the control surface is noted **δ** and its value is 5°. The control derivatives of the aerodynamic coefficients relative to the deflection of the control surface (C* δ) are defined as the difference value at some deflection angle minus the value at zero deflection angle divided by the deflection angle in radians. Table 4 summarises the control derivative results.

Mach number	***Angle of attack***	***Configuration***	***Cl δ***	***Cn δ***
0.2	9°	Winglet	-0.0075	0.0094
0.85	3°	Winglet	-0.0082	0.0151

Table 4 VELA2 configuration – Winglet's control surface efficiency

A positive deflection of the control surface implies a negative increment of the rolling moment and a positive increment of the yawing moment, in other words it forces the right wing to move upward and rearward. It should be noticed that starting a coordinated turn requires the rolling moment derivative and the yawing moment derivative to have the same sign. A left turn for example requires the wing to move up and forward, that is to say negative rolling moment and negative yawing moment. Here both roll and yaw control derivatives have almost the same magnitude and have opposite signs, so starting a coordinated turn with only the control surfaces of the winglets seems impossible at high and low speed conditions.

In addition, the magnitude of both rolling moment and yawing moment control derivatives is very small when compared to the corresponding lateral derivative relative to the sideslip angle. For the rolling moment control derivative, its low level can be explained by the fact that the additional rolling moment due to the deflection of the control surface results mainly from the normal force on the winglet and has a short arm relative to the reference point, while the rolling moment lateral derivative due to sideslip results mainly from the natural roll stability of a swept back wing. The yawing moment control derivative results both from the normal force on the winglet and from the drag of the winglet. The differential normal force has a large magnitude and a short arm while the differential drag force has a low magnitude and a large arm. This explains the low level of the yawing moment control derivative. If more yaw control is desired, maybe a split flap or a "crocodile" flap is preferable rather than a plain flap to obtain more differential drag between the left winglet and the right winglet.

2.5 Conclusions on the winglet efficiency

A winglet was defined and numerically optimised for the VELA 2 flying wing configuration in order to evaluate the lateral control potential of a control surface put on the winglet. A performance evaluation was realised using Euler computations and the far-field drag breakdown method while a rough estimation of the viscous drag was obtained using the flat plate boundary layer theory. It was shown that substantial drag reduction could be obtained from the winglet in transonic cruise conditions and landing or take-off conditions, but it must be kept in mind that the winglet is not adapted for low speed conditions. The analysis also proved than the winglet improves the lateral stability, both for roll and yaw. But if all wing-body configurations without central fins on the body and with winglets at the wing tips are stable in roll, they remain unstable in yaw at low speed conditions. Central fins on the body are needed at low speed conditions. In transonic cruise conditions, the lateral control obtained from a plain flap on the winglet does not allow starting a coordinated turn because the roll and yaw control derivatives have opposite signs, at low and high speed conditions.

3 Aerodynamic design of the AVECA flying wing configuration

3.1 Context

The AVECA configuration is a blended wing body of smaller capacity than the usual flying wing configurations studied during the past years at ONERA [1-2]. Work was carried out on this configuration within the framework of the French national project AVECA (ONERA-Airbus technical cooperation) which aims at designing viable flying wing configurations in cruise conditions while respecting strong geometric constraints such as cabin, cargo hold or landing gear volumes. The second part of this paper presents some results of this project and notably the aerodynamic design realised by ONERA, on the AVECA configuration, from an initial shape provided by Airbus.

In order to improve the aerodynamic performance of the initial configuration and to prescribe the final objectives of the design, a reliable evaluation of this performance was done in cruise conditions (M=0.85, Re/c=172.2 10^6). Thus, a Navier-Stokes multiblock structured mesh was realised. It is made up of 6 blocks for 2.6 10^6 points. The ONERA *elsA* software was used to carry out the CFD computations and the ONERA far-field drag extraction code, ffd used to evaluate the total drag and determine the different drag components. The ONERA far-field drag extraction approach allows the elimination of a large amount of the spurious drag due to numerical errors [5-7].

3.2 Objectives

The analysis of the results on the initial configuration shows that the location of the centre of pressure of this initial configuration is located in a position too far from the centre of gravity and would therefore results in a significant trim drag penalty. Indeed, it is located at 35% of the mean aerodynamic chord whereas the targeted value (corresponding to the estimated mean centre of gravity position) is at 40%. So the first objective of the design work was to move this centre of pressure downstream to reach the targeted position at the design point (M=0.85, Re/c=172.2 10^6 and a fixed lift coefficient). The second objective was to increase the lift-to-drag ratio at this design point. Finally, the third objective was to increase the margin against severe transonic flow feature by adapting the pressure surface distribution in order to avoid strong shock waves and strong isentropic Mach number values on both sides of the wing. These objectives had to be reached without violating the different geometric constraints (figure 5: cabin volume in blue and cargo hold volume in red).

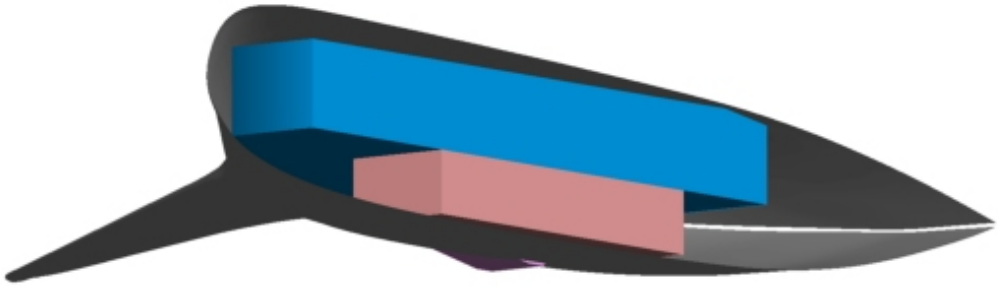

Figure 5 AVECA project – Geometric constraints

3.3 Methodology and geometry deformation

To reach these objectives, the different steps of the design consisted in applying modification of the wing section profiles at several control sections (located at fixed spanwise positions) defined on the inboard and outboard wing, while keeping the planform of the configuration unchanged. The manual design process was starting by modifying the inboard section of the configuration, and progressively moving to the outer section of the wing.

For the inboard part, four control sections were defined as shown in figure 6. In each section, seven control points were introduced and the section geometry was modified by prescribing local displacements on these different points. The modifications of the geometry were imposed directly on the mesh of the initial configuration. On each point of this mesh, the local displacements were determined using B-Spline curves defining from the displacements prescribed on the control points. For the outboard part of the wing, four control sections were also defined as shown in figure 6, in order to optimise the twist law of the wing without modifications of the shape of the wing in the different control sections.

For the design of the inboard part, a manual and iterative strategy was used whereas for the outboard part, an optimisation method was chosen to define the twist law of the configuration. This optimisation was driven by the gradient algorithm CONMIN. The total drag was defined as the function to be minimized considering constraints of the lift and on the location of the centre of pressure.

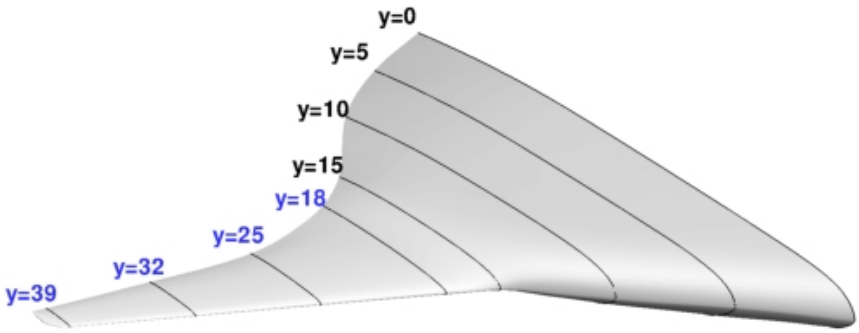

Figure 6 AVECA project – Definition of the control sections for the aerodynamic design of the inboard (in black) and outboard (in blue) parts of the wing.

3.4 Aerodynamic design

3.4.1 Design of the inboard wing

The first objective was to move the centre of pressure of the configuration downstream at the design point, that is to increase the rear load of the configuration. For this, the shape of the rear pressure side of the inboard wing was modified in the four control sections as shown in figure 7. This modification corresponds to a camber deformation.

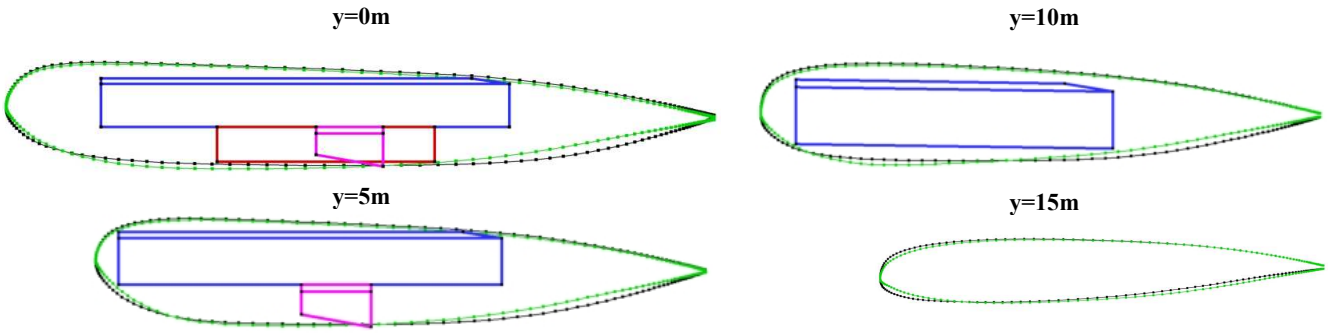

Figure 7 AVECA project – Aerodynamic design of the inboard wing (black: initial shape, green: final shape)

The different steps of the design showed a very strong sensitivity of the position of the centre of pressure to this modification. To obtain the better compromise between the different objectives, the final shape was defined in order to respect the trim of the configuration and to avoid the production of shock waves. This was made thanks to a limitation of the curvature on the rear part of the pressure side. In order to improve the efficiency of this modification, the thickness of the different sections was increased upstream. Thus, the curvature on the rear part of the pressure side remains very low in comparison with the one observed on the initial configuration in the three first control sections. These geometric modifications have a strong influence on the pressure distributions as shown in figures 8 and 9. Indeed, the shocks waves which can be observed on the initial configuration were completely suppressed on the final one.

The last modifications on the inboard wing concern the leading edge area, where the thickness was decreased to limit the maximum isentropic Mach number value on the suction side but also to decrease the viscous pressure drag of the configuration. Finally, the complete design of the inboard wing of the final configuration required about 60 configurations to be evaluated and compared using the elsA and ffd codes in a coarsened mesh of 600,000 points. Intensive use of the far-field drag extraction method allowed identifying the most critical regions which were contributing the most significantly to the different physical drag components (wave, induced and viscous components).

3.4.2 Design of the outboard wing

The second stage of the design aimed at optimising the twist law of the outboard wing in order to refine the longitudinal trimming of the configuration and to improve the lift-to-drag ratio at the design point. Five parameters were defined for the optimisation, the twist value in the four control sections and the angle of attack of the configuration. The position of the centre of pressure and the lift were defined as a constraint and the total drag as the function to be minimised.

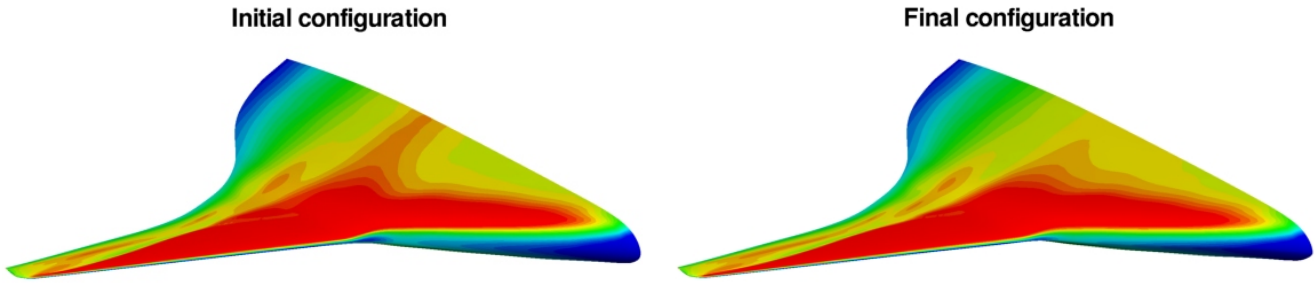

Figure 8 AVECA project – Pressure distributions on the suction side of the wing

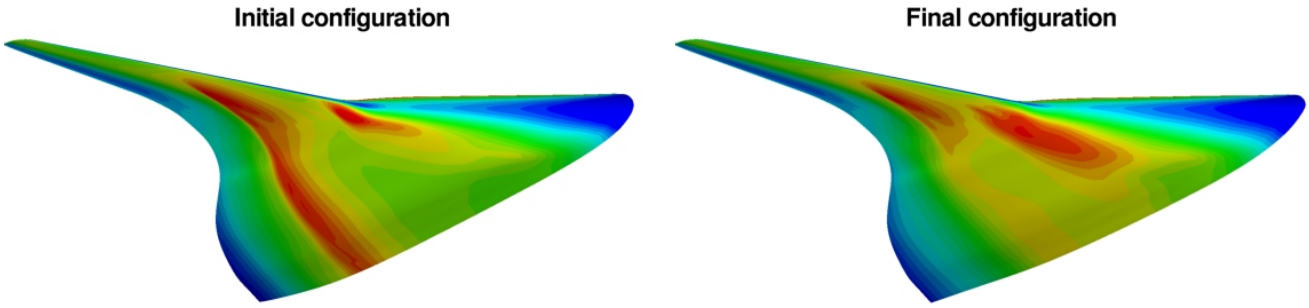

Figure 9 AVECA project – Pressure distributions on the pressure side of the wing

3.5 Performance analysis

3.5.1 Performance at the design point (M=0.85, $Re_{/c}$=172.2 10^6)

Figure 10 presents the aerodynamic performance of the initial and final configurations in terms of lift (CL in black), drag (CD in red), pitching moment (CM in blue) and lift-to-drag ratio (CL/CD in green) at the design point. The computations were carried out with the Navier-Stokes structured code *elsA* on the fine mesh (2.6 millions points) and the drag was evaluated using the ffd code.

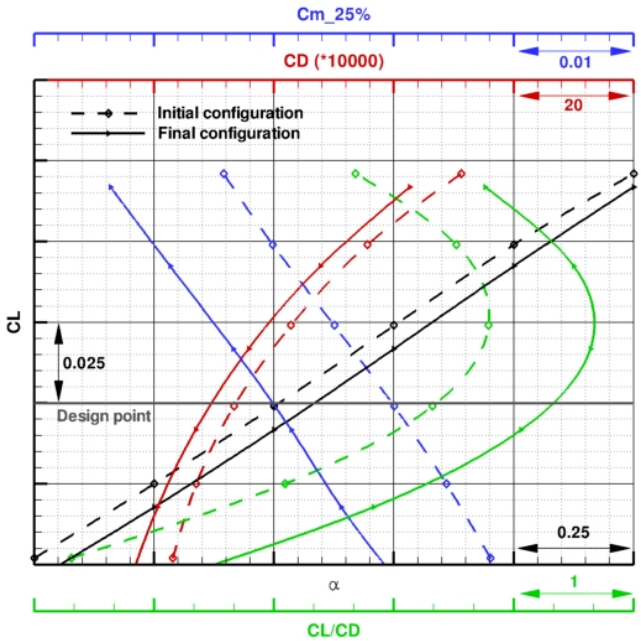

Figure 10 AVECA project – Aerodynamic performance at the design point

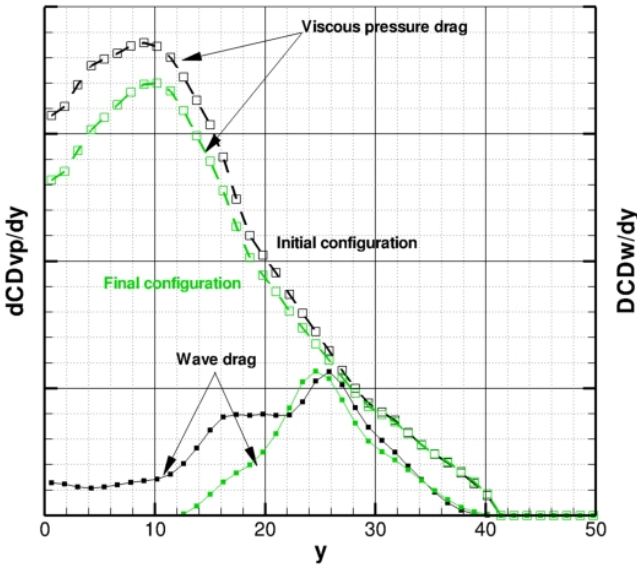

Figure 11 AVECA project – Spanwise drag distributions at the design point

First the evolution of the lift coefficient according the angle of attack α is similar for both configurations even if the gradient is slightly higher with the new configuration and if a little shift can be observed between both curves. For the pitching moment computed at the reference point located at 25% of mean aerodynamic chord, the shift of the curve translates the modification on the trim of the configuration. For the drag, a very important decrease is observed yielding to an increase of the lift-to-drag ratio of 1.0 at the design point and of 0.85 at the maximum value.

This analysis is supported by the spanwise distributions of viscous pressure and wave drag components (figure 11). Indeed the gain on the viscous pressure drag reaches 9.5% and 39.1% on the wave drag whereas the induced component remains unchanged. The decrease of the viscous pressure and wave drag components is especially important on the inboard wing.

3.5.2 Performance at M=0.87 ($Re_{/c}$=176.3 10^6)

The design was carried out for a design Mach number of 0.85, but the previous section has shown that the modifications on the geometry allow an important reduction of the wave drag sources. Consequently, the differences between the initial and final configurations in terms of lift-to-drag ratio are expected to grow with the Mach number. Figure 12 presents the performance of both configurations for a Mach number of 0.87.

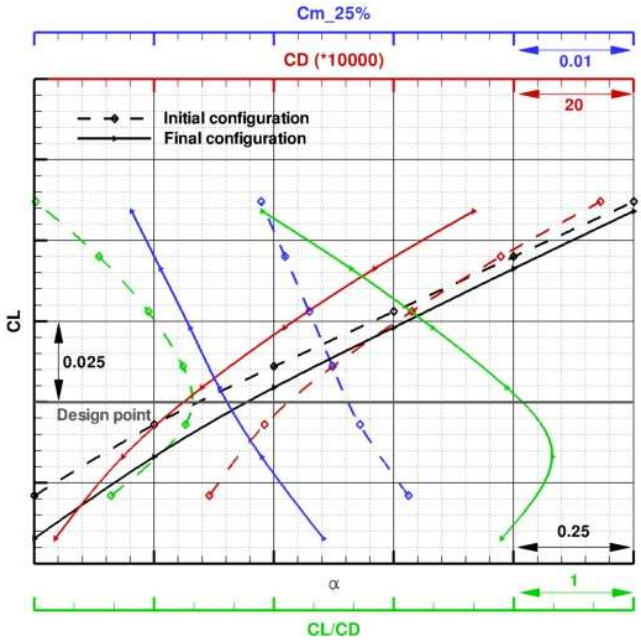

Figure 12 AVECA project – Aerodynamic performance at M=0.87

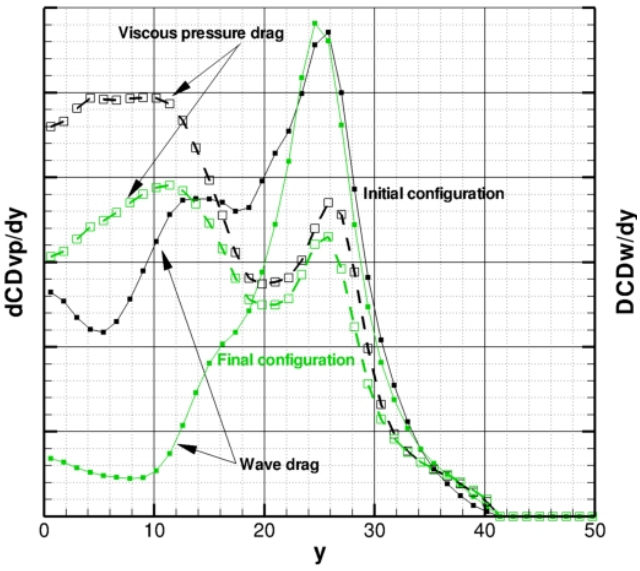

Figure 13 AVECA project – Spanwise drag distributions at M=0.87

For the lift-to-drag ratio, the difference reaches 3.0 at the design lift value between the initial and the final configurations. Moreover the lift value corresponding to the maximum lift to drag ratio decreases with the new configurations what translates important modifications on the aerodynamic behaviour of the configuration. The spanwise distributions in figure 13 confirm this analysis. A very important decrease of the viscous pressure and wave drag sources is observed on the inboard wing. The diminution of the wave drag component is about 37% and for the viscous pressure drag this value reaches 18.9%.

3.6 Conclusions on the AVECA configuration design

A new flying wing configuration was designed using an iterative strategy for the inboard wing and an automatic optimisation strategy for the outboard wing in cruise conditions (M=0.85). Very significant improvements were obtained in terms of longitudinal trimming and lift-to-drag ratio at cruise Mach number but also at higher Mach numbers thanks to the elimination of the main wave drag sources on the inboard wing.

4 Conclusions and prospects

In this paper, different aerodynamic design activities recently carried out by ONERA on flying wing configurations have been presented. First, within the framework the European NACRE project, the design of a blended winglet, equipped with a control surface on the VELA2 configuration, has demonstrated the efficiency of such a device to improve the aerodynamic performance (drag, control and lateral stability) of a flying wing configuration. Then, the aerodynamic design of a smaller capacity flying wing configuration carried out within the AVECA project resulted in encouraging cruise aerodynamic performance. Indeed, using an iterative strategy for the design of the inboard wing, a viable AVECA flying wing configuration has been defined under strong geometric constraints.

The ONERA-Airbus cooperation on this topic will be pursued within the AVECA project with the application of optimisation methods to automate the definition of new flying wing geometries using parametrisation suggested by the most influent design parameters identified with the iterative design strategy. These optimisations will be realised for several planforms of the AVECA flying wing configuration in order to study the trade-off and the sensitivity of drag coefficients to planform variations.

Acknowledgments

The work presented in the first part of this paper was partly funded by the European Commission under the FP6 Integrated Project NACRE, in cooperation with Airbus, DLR, FOI, PEDECE, TsAGI, VZLU and Warsaw University of Technology. The authors would also like to thank the French government agencies DGAC (Direction Générale de l'Aviation Civile) and DGA (Délégation Générale pour l'Armement) for the funding of the studies presented in the second part of this paper. The authors are also particularly thankful to B. Mialon for his work within the framework of the NACRE project.

References

[1] B. Mialon, T. Fol, C. Bonnaud. "Aerodynamic Optimization of Subsonic Flying Wing Configurations". 20th AIAA Applied Aerodynamics Conference, Saint Louis, USA, June 24-26 2002.

[2] B. Mialon, M. Hepperle. "Flying Wing Aerodynamics Studies at ONERA and DLR". CEAS Katnet Conference on Key Aerodynamic Technologies, Bremen, Germany, June 20-22 2005.

[3] G.N. Vanderplaats. "CONMIN – A Fortran Program for Constrained Function Minimisation - User's Manual". NASA – TMX No 62-282, August 1973.

[4] M.E. Leroy, G.N. Vanderplaats. "COPES – A Fortran Program for Engineering Synthesis". Naval Postgraduate School Monterey CA, Report No NPS69-81-003, March 1982.

[5] D. Destarac. "Far-Field / Near-Field Drag Balance Applications of Drag Extraction in CFD". VKI Lectures Series 2003, CFD-based Aircraft Drag Prediction and Reduction, National Institute of Aerospace, Hampton (VA), November 3-7, 2003.

[6] S. Esquieu. "Reliable Drag Extraction from Numerical Solutions: Elimination of Spurious Drag". Symposium, RTO-MP-AVT-147, Paper 42, Athens, Greece, December 3-6 2007.

[7] D. Destarac. "Drag Extraction from Numerical Solutions to the Equations of Fluid Dynamics: the Far-field Philosophy". 43ème Congrès d'Aérodynamique Appliquée de la 3AF, Maîtrise de la traînée et de l'impact sur l'environnement, Poitiers, France, March 10-12 2008.